

Analysis of Raman scattering from two-phonon bound states*

K. L. Ngai and A. K. Ganguly

Naval Research Laboratory, Washington, D. C. 20735

J. Ruvalds

Physics Department, University of Virginia, Charlottesville, Virginia 22901

(Received 25 March 1974)

The possible formation of a bound state of two phonons by repulsive anharmonic coupling has been previously discussed in terms of a simple model Hamiltonian. These theoretical efforts yield a reasonable estimate for the bound-state energy, and provide a physical interpretation for the observed anomalous peak in the two-phonon Raman spectrum of diamond. In the present paper we consider the Raman intensity attributed to scattering from two-phonon bound states. The present theory is based on a two-phonon deformation-potential approach. The calculated intensity for diamond is in good agreement with available experimental data and thus provides further evidence for the existence of bound phonon pairs.

I. INTRODUCTION

Cohen and Ruvalds¹ have recently proposed that anharmonic phonon-phonon interactions can give rise to two-phonon bound states. The anomalous sharp peak observed in the second-order Raman spectrum of diamond by Krishnan² and more recently by Solin and Ramdas³ was interpreted as evidence for the existence of bound states. The sharp peak resides at a frequency higher than twice the maximum single-phonon frequency. This feature is explained by the anharmonic interaction theory¹ in terms of the splitting of the bound phonon pair state off the two-phonon continuum as a result of the repulsive phonon-phonon interaction. From a comparison between experiment and theory of the "binding" energy, its anharmonic coupling strength in diamond has been deduced. The value of its anharmonic strength was shown to be plausible.¹ Experimental data on its anomalous sharp peak gives not only its "binding" energy, but also its Raman scattering intensity and line shape. In the initial theories^{1,4} on two-phonon bound states, the scattering-intensity aspect of the experimental data has not been examined and tested against the theoretical predictions.

One of the purposes of the present work is to calculate the scattering intensity of the two-phonon bound state and compare it with the experimental Raman data, thus providing an independent check on previous theories.^{1,4} It is now possible to consider this question because of the recent developments in the theory of electron-two-phonon deformation-potential interactions.⁵⁻⁷ A precise knowledge of these interaction matrix elements is required to provide quantitative analysis of the intensity of second-order light scattering.

The bound-state intensity is derived in Sec. II. In Sec. III we discuss the theory of second-order Raman scattering for the special case of diamond,

and relate the bound-state intensity of Sec. II to experiment.

II. TWO-PHONON BOUND STATES

In the following we extend the Ruvalds and Zawadowski⁴ treatment of interacting phonons to calculate the spectral weight function in terms of a simple model for the two-phonon density of states. The spectral function will enable us to calculate the Raman scattering intensity of the bound state.

It should be mentioned that the present formalism is applicable to calculations of the two-phonon continuum in the presence of anharmonic interactions. However, the structure within the continuum is complicated by Van Hove singularities arising from various critical points throughout the Brillouin zone. Furthermore, the anharmonic interactions distort the singular structure in a prominent way and may yield additional peaks in the spectrum corresponding to two-phonon resonances.

We focus attention on the bound-state formation since it gives rise to a very sharp peak outside the two-phonon continuum. This feature enables us to estimate the bound-state energy and line shape with exceptional accuracy. To our knowledge diamond is best for our purposes, since the experimental evidence for a true bound state is compelling and the single-phonon dispersion is well known from neutron scattering studies.⁸ The existence of a bound state of two acoustic phonons in quartz has also been invoked⁴ to explain the Raman data of Scott,⁹ which exhibits an interesting level repulsion between a soft optic phonon and the state of two acoustic phonons; this hybridization is analogous to the Fermi resonance of vibrational levels in molecular systems, but exhibits broadened structure owing to the substantial dispersion of the acoustic phonons and the finite lifetime of the soft mode.

We consider a model Hamiltonian of phonons described by

$$H_{\text{ph}} = \sum_{q,j} \omega_{qj} (b_{qj}^\dagger b_{qj} + \frac{1}{2}) + g_3 \sum'_{\substack{k_1, k_2, q \\ \text{all } j}} (b_{k_1 j_1}^\dagger b_{q j_2}^\dagger b_{k-q, j_3}^\dagger + \text{H. c.}) + g_4 \sum'_{\substack{k_1, k_2, q \\ \text{all } j}} b_{k_2 - q, j_1}^\dagger b_{k_1 + q, j_2}^\dagger b_{k_1, j_3} b_{k_2, j_4}, \quad (2.1)$$

where ω_{qj} is the frequency of the single optic phonon with polarization j , $b_{k,j}^\dagger$ is the creation operator for this phonon, and g_3 and g_4 are momentum-independent anharmonic-coupling parameters. Since we are considering the optic modes of diamond, the usual phonon branch index is suppressed, and it is reasonable to approximate the microscopic anharmonic coupling¹⁰ by constant parameters g_3 and g_4 .⁴ The prime on the summations excludes phonon combinations forbidden by symmetry.

The two-phonon Green's function $G_2(Q, \omega)$ has been obtained in Ref. 4. Here we denote by Q , the sum $\vec{k} + \vec{k}'$ of the momenta of two phonons. For second-order Raman scattering considerations, we can take $\vec{Q} = 0$ since the wave vectors of both incident and scattered photons are negligible. The Green's function for a pair of noninteracting phonons with polarizations j_1 and j_2 is given by⁴

$$F_{j_1 j_2}(\omega) = \frac{i}{(2\pi)^4} \int d^3 q \int d\bar{\omega} G_{1j_1}(q, \omega - \bar{\omega}) G_{1j_2}(-q, \bar{\omega}), \quad (2.2a)$$

which reduces to

$$F_{j_1 j_2} = \frac{1}{(2\pi)^3} \int \frac{d^3 q}{\omega - \omega_{qj_1} - \omega_{-qj_2} + i(\Gamma_{qj_1} + \Gamma_{-qj_2})} \quad (2.2b)$$

or, equivalently,

$$F_{j_1 j_2} = \frac{\rho_{2, j_1 j_2}(\omega') d\omega'}{\omega - \omega' + 2i\Gamma}. \quad (2.2c)$$

Here G_{1j} denotes the one-phonon Green's function, and the single-phonon width Γ is taken to be same for all branches. Thus the effects of the phonon dispersion are conveniently included in the joint phonon density of state $\rho_{2, j_1 j_2}$.

To calculate the bound-state formation, we calculate the multiple scattering of two LO phonons as shown in Fig. 1. Considering our model Hamiltonian, the multiple scattering series is summed trivially and yields the coupled two-phonon Green's functions,

$$G_2^{LL} = \frac{F_L(\omega)}{1 - g_4 [F_L(\omega) + 2F_T(\omega)]} \quad (2.3a)$$

and

$$G_2^{TT} = \frac{F_T(\omega)}{1 - g_4 [F_L(\omega) + 2F_T(\omega)]}. \quad (2.3b)$$

Here the two-LO-phonon coupling to the TO-phonon pair is allowed by symmetry and the factor of 2 takes into account the two polarizations of the transverse optic phonons. The criterion for the formation of a bound pair of two phonons is the existence of a pole in the two-phonon propagator, i. e.,

$$1 - g_4 [F_L(\omega) + 2F_T(\omega)] = 0, \quad (2.4)$$

with ω outside the two-phonon continuum. Thus the observed bound states may include contributions from both LO and TO branches, although their relative strengths will generally be different.

Providing that the anharmonic coupling g_4 is sufficiently strong, the two-phonon spectral function $\rho_{2, j_1 j_2} = -\pi^{-1} \text{Im} G_2^{j_1 j_2}(\omega)$ will exhibit a bound-state component split off from the $j_1 j_2$ phonon pair continuum which is of the form

$$\rho_{2, j_1 j_2}^B(\omega) = Z_{j_1 j_2} \delta(\omega - \omega_B), \quad (2.5)$$

where the bound-state energy is determined by solutions to Eq. (2.4).

In actual situations the bound-state peak may be broadened somewhat by the single-phonon lifetime. Nevertheless, the intensity of the peak is easy to determine from Eqs. (2.3a) and (2.3b), and is given by

$$Z_{j_1 j_2} = \left[g_4^2 \frac{\partial}{\partial \omega} [F_L(\omega) + 2F_T(\omega)] \right]_{\omega=\omega_B}^{-1}. \quad (2.6)$$

To this point the formalism is applicable to situations described by a completely general density of states $\rho_2(\omega)$.

Detailed information on the single-phonon dispersion curves of diamond can be obtained from the neutron scattering data of Warren *et al.*⁸ We shall rely heavily on their data to justify several approximations that will be made here. Consider first the LO branch. Its dispersion is rather flat in a large region of the Brillouin zone, and hence $\rho_{2, LL}^{(0)}(\omega)$ should be well approximated by a step function extending over a bandwidth $2D$, in other words,

$$\begin{aligned} \rho_{2, LL}^{(0)}(\omega) &= A_L \text{ for } 2\omega_m - 2D_L < \omega < 2\omega_m \\ &= 0 \text{ elsewhere,} \end{aligned} \quad (2.7)$$

where ω_m is the maximal single-phonon frequency.

The product $2D_L A_L$ must be equal to N_s , the total number of LO-phonon states in the entire Brillouin zone and is a constant. Then it follows from Eqs. (2.2c), (2.4), and (2.6) that

$$F_{LL}(\omega) = A_L \ln \left| \frac{\omega - 2\omega_m}{\omega - 2\omega_m + 2D_L} \right| + i\rho_{2,LL}^{(0)}. \quad (2.8)$$

For the TO phonons we make the similar approximations for the density of states as in Eq. (2.6), but with smaller height A_T and corresponding larger bandwidth $2D_T$. From Eqs. (2.4) and (2.8) the bound-state energy in the weak-coupling limit $E_B = \omega_B - 2\omega_m \ll D_L$ becomes

$$\omega_B = 2\omega_m + 2D_L \exp(-1/g\xi A_L), \quad (2.9)$$

where ξ takes into account the TO-phonon contribution and is given by

$$\xi = 1 + \frac{2D_L \ln(E_B/2D_T)}{D_T \ln(E_B/2D_L)}. \quad (2.10)$$

Similarly, the bound-state strength defined in Eq. (2.5) follows from Eqs. (2.6), (2.8), and (2.9) and is

$$Z_{LL} = \frac{\xi E_B N_s}{4D_L} \left[\ln \left(\frac{2D_L}{E_B} \right) \right]^2. \quad (2.11)$$

Similarly the TO branches yield

$$Z_{TT} = Z_{LL} \frac{F_T(\omega_B)}{F_L(\omega_B)} = Z_{LL} \left(\frac{\xi - 1}{2} \right). \quad (2.12)$$

There the total strength of the bound state including both longitudinal and optical branches is

$$Z_{\text{total}} = Z_{LL} + 2Z_{TT} = \xi Z_{LL}. \quad (2.13)$$

In the case of diamond, the neutron data⁸ yield $D_L \approx 150 \text{ cm}^{-1}$ and $D_T \approx 300 \text{ cm}^{-1}$, and the Raman data³ give $E_B \approx 1 \text{ cm}^{-1}$. Inserting these values in the above formulas we estimate the bound-state strength in diamond to be

$$Z_{\text{total}} \approx 0.24 N_s, \quad (2.14)$$

where $3N_s$ denotes the total density of states included in the continuum portion of $\rho_{2LL}^{(0)} + \rho_{2TT}^{(0)}$.

The Raman spectrum of diamond³ indicates that the observed bound-state peak has primarily Γ_1^+ symmetry and therefore may include contributions from overtones of LO and TO phonons. However, to make a comparison of the above results with the observed spectrum in diamond, we need to consider the theory of second-order Raman scattering. This analysis for the special case of diamond is discussed in the following section.

III. RAMAN SCATTERING FROM TWO-PHONON STATES

In this section we shall present a theory of second-order Raman scattering. The Raman scattering cross section is expressed in terms of the two-phonon deformation potentials and the two-phonon

Green's function. The theory is applicable to both the two-phonon continuum and bound states. This enables us to calculate the ratio of the scattering intensities from the two-phonon bound state to the continuum.

In second-order Raman scattering an incident photon in state $\omega_{\vec{\chi}, \vec{\epsilon}}$ ($\omega_{\vec{\chi}, \vec{\epsilon}}$ is the frequency, $\vec{\chi}$ the wave vector, and $\vec{\epsilon}$ the polarization vector) is scattered into the state $\omega_{\vec{\chi}', \vec{\epsilon}'}$ with the emission of two phonons with total momentum $Q=0$. From Loudon's theory,¹¹ photon-phonon coupling occurs indirectly through the intermediary of electron-phonon and electron-phonon interactions. The direct interaction between photons and phonons is negligible when $\omega_{\vec{\chi}, \vec{\epsilon}} \gg \omega_{\vec{q}, \vec{s}, j}$.

We shall restrict our considerations to the group-IV homopolar insulators having the diamond lattice structure. In the case of homopolar materials the only source of electron-lattice interaction is the perturbation of the periodic potential acting on electrons produced by the displacement of the atoms of the lattice. For lattices with two atoms per unit cell this deformation-potential interaction between electrons and phonons can be written, up to second order in atomic displacements, (for Stoke's scattering only) as

$$H_{ep} = H_{ep}^{(1)} + H_{ep}^{(2)}, \quad (3.1)$$

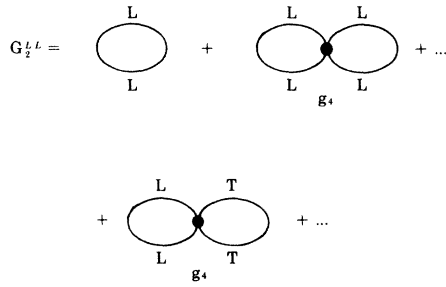
where

$$H_{ep}^{(1)} = \sum_{\vec{q}, \vec{s}, j_1} \sum_{n\vec{k}, n'\vec{k}'} \left(\frac{\hbar}{2MNa^2 \omega_{\vec{q}\vec{s}j_1}} \right)^{1/2} \times \langle n'\vec{k}' | \vec{e}_j \cdot \vec{D}^{(1)}(\mathbf{r}) | n\vec{k} \rangle b_{\vec{q}\vec{s}j_1}^\dagger a_{n'\vec{k}'}^\dagger a_{n\vec{k}} a_{\vec{q}\vec{s}j_1} \delta_{\vec{k}' - \vec{k}, \vec{q}} \quad (3.2)$$

and

$$H_{ep}^{(2)} = \sum_{\vec{q}, \vec{s}, j_1} \sum_{\vec{q}', \vec{s}', j_2} \sum_{n\vec{k}, n'\vec{k}'} \frac{\hbar}{2MNa^2 (\omega_{\vec{q}, \vec{s}, j_1} \omega_{\vec{q}', \vec{s}', j_2})^{1/2}} \times \langle n'\vec{k}' | \vec{e}_{j_1} \cdot \vec{D}^{(2)} \cdot \vec{e}_{j_2} | n\vec{k} \rangle b_{\vec{q}\vec{s}j_1}^\dagger b_{\vec{q}'\vec{s}'j_2}^\dagger a_{n'\vec{k}'}^\dagger a_{n\vec{k}} \delta(\vec{k}' - \vec{k}, \vec{q} + \vec{q}'). \quad (3.3)$$

We neglect the effects of the anharmonic interactions on the form of the electron coupling. Here $\omega_{\vec{q}\vec{s}j_1}$ is the phonon frequency, M is the reduced mass of the two atoms in the unit cell, N is the number of unit cells, and a is the lattice constant. The one- and two-optical-phonon deformation potentials $\vec{D}^{(1)}$ and $\vec{D}^{(2)}$ are given, respectively, by $\vec{D}^{(1)} + a\nabla_{\mathbf{u}} U_0$ and $\vec{D}^{(2)} = a^2 \nabla_{\mathbf{u}} \nabla_{\mathbf{u}} U_0$, where U_0 is the equilibrium lattice potential screened¹² by the bound electrons and $\vec{u} = \vec{u}_1 - \vec{u}_2$ the relative displacement of the two sublattices. $|n\vec{k}\rangle$ denotes Bloch state for the electrons in band n with quasimomentum \vec{k} . The deformation potential is short ranged and we will assume that the matrix elements of $\vec{D}^{(1)}$ and $\vec{D}^{(2)}$ are independent of wave vectors. a^\dagger (a) is the electron creation (annihilation) operator.



$$G_2^{L,L} = F_L [1 + g_4 (F_L + 2F_T) + \dots]$$

FIG. 1. Diagrammatic representation of two-phonon multiple scattering processes. The solid lines refer to LO phonons (L) and TO phonons (T), respectively, and the dot refers to the effective anharmonic coupling g_4 which is assumed to be independent of momentum. Note that the propagator $G_2^{L,L}$ for the LO phonons includes a spectral contribution from the transverse optical-phonon Green's function F_T to all orders in the coupling.

The electron-photon interaction is given by

$$H_{eR} = \sum_{\vec{x}, \vec{\sigma}} \sum_{\vec{n}\vec{k}, \vec{n}'\vec{k}'} \frac{e}{m^*} \left(\frac{\hbar}{V\epsilon_\infty\omega\vec{x}\vec{\sigma}} \right)^{1/2} \langle n'\vec{k}' | \vec{\epsilon} \cdot \vec{p} | n\vec{k} \rangle \times (A_{\vec{x}, \vec{\sigma}} + A_{-\vec{x}, \vec{\sigma}}^\dagger) a_{n', \vec{k}'}^\dagger a_{n, \vec{k}} \delta(\vec{k} - \vec{k}', \vec{\chi}), \quad (3.4)$$

where V is the volume of the crystal and ϵ_∞ the high-frequency dielectric constant; e is the electronic charge, m^* the effective mass of the electrons, \vec{p} the momentum operator of electrons and $A (A^\dagger)$ the annihilation (creation) operators for photons. We will neglect the wave-vector dependence of the matrix elements of the dipole-moment operator.

Second-order Raman scattering can occur via three types of processes as shown in Fig. 2. In processes of the type depicted in Fig. 2(a), the two phonons are emitted simultaneously owing to the second-order interaction $H_{ep}^{(2)}$ between electrons (holes) and phonons. There are six possible time orderings of the three interactions involved. In processes of Fig. 2(b), the two phonons are emitted separately owing to the first-order electron (hole)-phonon interaction $H_{ep}^{(1)}$ acting twice through intermediate states. There are 24 possible time orderings for these processes. Processes of Fig. 2(c) involve higher-order electron-photon interaction and can be neglected. The initial state $|i\rangle$ of the system will consist of n_1 incident photons, no scattered photon, $n_{\vec{q}\vec{\sigma}j_1}$ and $n_{\vec{q}\vec{\sigma}j_2}$ phonons in their ground state. The final state $|f\rangle$ will have $n_1 - 1$ incident photons, one scattered photon, $n_{\vec{q}\vec{\sigma}j_1} + 1$ and $n_{\vec{q}\vec{\sigma}j_2} + 1$ phonons and electrons in their ground state. In the electronic ground state the valence bands are full and the conduction bands are empty. The differential cross section

for scattering from the initial state $|i\rangle$ to final state $|f\rangle$ is given by¹³

$$\frac{d\sigma}{d\Omega d\omega} = \frac{\chi_s \epsilon_\infty^{1/2}}{\hbar c} \sum_f |\langle f | T | i \rangle|^2 \delta(\omega - \Omega_i + \Omega_f), \quad (3.5)$$

where T is the scattering matrix and c the velocity of light in vacuum. The wave vectors and frequencies of the incident and scattered photons are respectively $(\vec{\chi}_i, \omega_i)$ and $(\vec{\chi}_s, \omega_s)$; $\omega = \omega_i - \omega_s$ is the frequency transfer to the phonon system. The energies of the initial and final phonon states are denoted, respectively, by $\hbar\Omega_i$ and $\hbar\Omega_f$. The scattering T matrix may be written as

$$T = H_{int} + H_{int} \frac{1}{E_i - H_0} H_{int}. \quad (3.6)$$

Here E_i is the energy in the initial state $|i\rangle$, H_{int} is the perturbation $H_{eR} + H_{ep}^{(1)} + H_{ep}^{(2)}$, and H_0 the unperturbed Hamiltonian of the electrons, photons, and phonons (including the fourth-order anharmonic interactions). The anharmonic interactions between phonons, the g_4 term in Eq. (2.1), is included to all orders because of the bound state.

Second-order Raman scattering arises from the third and the fourth terms in Eq. (3.6). The matrix elements of T will involve all intermediate electron-hole states. However, we will consider only the highest valence band and the lowest con-

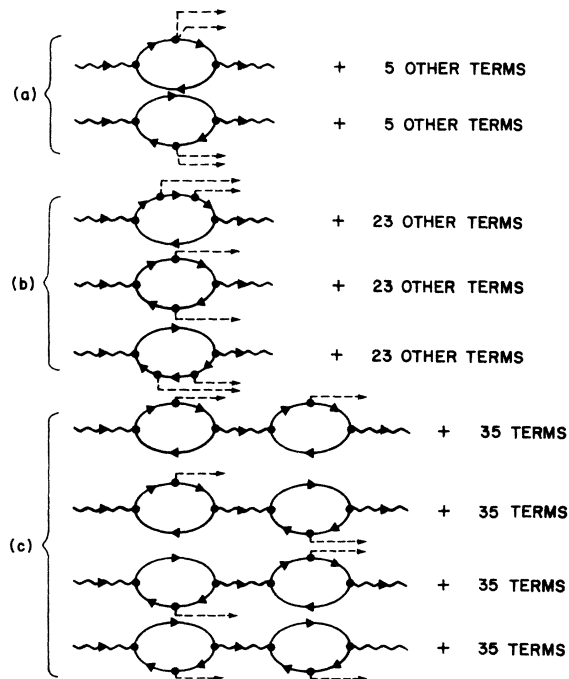


FIG. 2. Diagrams of the three types of processes contributing to the two-phonon Raman scattering: The photon line is wavy. The electron (hole) line is straight. The phonon line is dotted.

duction band. The contributions from all other higher bands will be small owing to the energy denominators in Eq. (3.6). Furthermore, in this paper we deal with nonresonant Raman scattering where the energy of the incident photon is less than the energy gap. Hence the intermediate electronic states will be taken as free electron-hole pairs and the excitonic and polariton effects¹⁴ will be neglected.

In systems with a center of inversion, the electronic states will have definite parity. Therefore the intraband matrix elements of the electron-momentum operators will be zero. Thus in the two-band model used here, only two terms from Fig. 2(a) and four terms from Fig. 2(b) will survive. These are the diagrams where the initial and the final vertices represent electron-photon interac-

tions. Thus the relevant part of the T matrix is

$$T = H_{eR} \frac{1}{E_I - H_0} \left(H_{ep}^{(2)} + H_{ep}^{(1)} \frac{1}{E_I - H_0} H_{ep}^{(1)} \right) \frac{1}{E_I - H_0} H_{eR}. \quad (3.7)$$

Interference between the matrix elements of $H_{ep}^{(2)}$ and $H_{ep}^{(1)}[1/(E_I - H_0)] H_{ep}^{(1)}$ is generally important and an effective two-phonon-electron deformation potential interaction may be defined⁵⁻⁷ as

$$H_2^{eff} = H_{ep}^{(2)} + H_{ep}^{(1)} \frac{1}{E_I - H_0} H_{ep}^{(1)}. \quad (3.8)$$

From Eqs. (3.5) and (3.7) on substituting for $H_{ep}^{(2)}$ and $H_{ep}^{(1)}$ from Eqs. (3.2) and (3.4) and using the integral representation for $\delta(\omega - \Omega_i + \Omega_f)$, we have

$$\begin{aligned} \frac{d\sigma}{d\Omega d\omega} &= \frac{e^4 \omega_i \omega_s^3}{4\hbar^2 M^2 N^2 m^{*4} c^4} \sum_{\substack{q\epsilon j_1 \\ q'\epsilon' j_2}} \delta(\vec{\chi}_i - \vec{\chi}_s, \vec{q} + \vec{q}') \frac{|R_{\epsilon\epsilon'}^{j_1 j_2}(\omega_i, \omega_s)|^2}{\omega_{q\epsilon j_1} \omega_{q'\epsilon' j_2}} \\ &\times \frac{1}{2\pi} \int_{-\infty}^{\infty} e^{i(\omega - \Omega_i + \Omega_f)t} \langle i | b_{q\epsilon j_1} b_{q'\epsilon' j_2} | f \rangle \langle f | b_{q\epsilon j_1}^\dagger b_{q'\epsilon' j_2}^\dagger | i \rangle dt, \end{aligned} \quad (3.9)$$

where $|i\rangle$ and $|f\rangle$ refer respectively to the initial and final phonon states. The two states differ in the occupation numbers $\vec{q}\epsilon j_1$ and $\vec{q}'\epsilon' j_2$. In Eq. (3.9) the second-order Raman tensor is given by

$$R_{\epsilon\epsilon'} = \frac{\hbar^2}{\omega_i \omega_s V} \sum_{\vec{k}} \left(\frac{\langle v | \vec{\epsilon} \cdot \vec{p} | c \rangle D \langle c | \vec{\epsilon}' \cdot \vec{p} | v \rangle}{(E_{\vec{k}\vec{k}}^{(cv)} - \hbar\omega_s)(E_{\vec{k}\vec{k}}^{(cv)} - \hbar\omega_i)} + \frac{\langle v | \vec{\epsilon} \cdot \vec{p} | c \rangle D \langle c | \vec{\epsilon}' \cdot \vec{p} | v \rangle}{(E_{\vec{k}\vec{k}}^{(cv)} + \hbar\omega_i)(E_{\vec{k}\vec{k}}^{(cv)} + \hbar\omega_s)} \right). \quad (3.10)$$

Here $E_{\vec{k}\vec{k}}^{(cv)}$ is the energy of electron-hole pair which under parabolic approximation can be written as $E_{\vec{k}\vec{k}}^{(cv)} = E_g + \hbar^2 k^2 / 2\mu + \hbar^2 K^2 / 2(m_e^* + m_h^*)$, E_g being the band gap and μ the reduced electron-hole mass and c (v) refers to conduction (valence) bands. D is the matrix element of the effective two-phonon deformation potential given by

$$\begin{aligned} D &= \langle c | \vec{\epsilon}_{j_1} \cdot \vec{D}^{(2)} \cdot \vec{\epsilon}_{j_2} | c \rangle - \langle v | \vec{\epsilon}_{j_1} \cdot \vec{D}^{(2)} \cdot \vec{\epsilon}_{j_2} | v \rangle \\ &+ \frac{(\langle c | \vec{\epsilon}_{j_1} \cdot \vec{D}^{(1)} | c \rangle - \langle v | \vec{\epsilon}_{j_1} \cdot \vec{D}^{(1)} | v \rangle)(\langle c | \vec{\epsilon}_{j_2} \cdot \vec{D}^{(1)} | c \rangle - \langle v | \vec{\epsilon}_{j_2} \cdot \vec{D}^{(1)} | v \rangle)}{E_{\vec{k}\vec{k}}^{(cv)} - \hbar\omega_i - \hbar\omega_s}. \end{aligned} \quad (3.11)$$

In Eqs. (3.10) and (3.11) the energy denominators should contain the renormalized phonon frequencies. Since the corrections to the frequencies are small and $(E_g - \hbar\omega)$ is much larger than the phonon frequencies, the error incurred by the use of unrenormalized frequencies is small. In this approximation the two-phonon deformation potential is the same for both bound and free phonon pairs.

In Eq. (3.9) we transform the operators $b^\dagger(b)$ to Heisenberg representation

$$e^{-i(\Omega_i - \Omega_f)t} \langle f | b_{q\epsilon j_1}^\dagger b_{q'\epsilon' j_2}^\dagger | i \rangle = \langle f | e^{iH_p t} b_{q\epsilon j_1}^\dagger e^{-iH_p t} e^{iH_p t} b_{q'\epsilon' j_2}^\dagger e^{-iH_p t} | i \rangle = \langle f | b_{q\epsilon j_1}^\dagger(t) b_{q'\epsilon' j_2}^\dagger(t) | i \rangle, \quad (3.12)$$

and using the relation $\sum_f |f\rangle\langle f| = 1$ we get for the scattering cross section

$$\frac{d\sigma}{d\Omega d\omega} = \frac{e^4 \omega_i \omega_s^3}{4\hbar^2 M^2 N^2 m^{*4} c^4} \sum_{\substack{q\epsilon j_1 \\ q'\epsilon' j_2}} \delta(\vec{\chi}_i - \vec{\chi}_s, \vec{Q}) \frac{R_{\epsilon\epsilon'}^{j_1 j_2}(\omega_i, \omega_s)}{\omega_{q\epsilon j_1} \omega_{q'\epsilon' j_2}} \frac{1}{2\pi} \int_{-\infty}^{\infty} dt e^{i\omega t} \langle\langle b_{q\epsilon j_1}(0) b_{q'\epsilon' j_2}(0) b_{q\epsilon j_1}^\dagger(t) b_{q'\epsilon' j_2}^\dagger(t) \rangle\rangle, \quad (3.13)$$

where $\langle\langle \rangle\rangle$ denotes thermal average and $\vec{Q} = \vec{q} + \vec{q}'$. Since $\vec{\chi}_i - \vec{\chi}_s \approx 0$ we will assume that $\vec{Q} = 0$. If the phonon frequencies in the denominator of Eq. (3.13) are taken independent of \vec{q} and replaced by some average values, then the sum \vec{q} can be taken inside the integral. The integral is then related to the imaginary part of

the Fourier transform of the two-phonon retarded Green's function¹⁵ defined in Sec. I, i. e.,

$$\frac{1}{2\pi} \int_{-\infty}^{+\infty} dt e^{i\omega t} \sum_{\vec{q}} \langle \langle b_{\vec{q},j}(0) b_{-\vec{q},j}(0) b_{\vec{q},j}^{\dagger}(t) b_{-\vec{q},j}^{\dagger}(t) \rangle \rangle = \frac{-1}{\pi} (n_{\omega_j} + 1)^2 \text{Im} G_{\vec{R}}^{(2)}(\vec{Q} = 0, \omega) = (n_{\omega_j} + 1)^2 \rho_{2,jj}(\vec{Q} = 0, \omega), \quad (3.14)$$

where n_{ω_j} is the single-phonon Bose factor ($e^{\hbar\omega_j/kT} - 1$)⁻¹ and $\rho_{2,jj}(\vec{Q} = 0, \omega)$ is the two-phonon joint density of states such that the total wave vector $\vec{Q} \approx 0$ and the two-phonon energy (ω) is equal to $\omega_i - \omega_s$. $\rho_{2,jj}$ can be written as the sum of contributions from the continuum and bound states:

$$\rho_{2,jj}(\omega) = \rho_{2,jj}^{(c)}(\omega) + \sum_j Z_{jj} \delta(\omega - \omega_{jj}). \quad (3.15)$$

We then obtain for the scattering cross section for the two-phonon bound state

$$\left(\frac{d\sigma}{d\Omega} \right)_{\text{bound}} = \frac{e^4 \omega_i \omega_s^3}{4 \hbar^2 M^2 N (m^* a c)^4} \sum_j \frac{Z_{jj} (n_{\omega_j} + 1)^2}{\omega_j^2} |R_{\vec{q}\vec{q}'}| \quad (3.16)$$

and for the continuum phonon states

$$\left(\frac{d\sigma}{d\Omega} \right)_c = \frac{e^4 \omega_i \omega_s^3}{4 \hbar^2 M^2 N (m^* a c)^4} \sum_j |R_{\vec{q}\vec{q}'}(\omega_i, \omega_s)|^2 \times \int \frac{(n_{\omega_j} + 1)^2}{\omega_j^2} \rho_{2,jj}^{(c)}(\omega) d\omega. \quad (3.17)$$

In Eq. (3.17) we make the approximation that $R_{\vec{q}\vec{q}'}$ and ω_s^3 are slowly varying functions of frequency and can be taken outside the integral. This will be particularly true for optic phonon branches with small bandwidth. We also neglect the kinetic energy of the center-of-mass motion of the electron-hole pair in the expression for $R_{\vec{q}\vec{q}'}$, since $\vec{\chi} \approx 0$ and $\vec{\chi}' \approx 0$. The assumption that the deformation potentials⁹ for bound and continuum phonons do not differ can be justified because the bound-state formation involves anharmonic interactions small compared with electronic energies. On replacing the $\sum_{\vec{q}}$ in Eq. (3.10) by an integral, we have an explicit expression for $R_{\vec{q}\vec{q}'}$ as

$$R_{\vec{q}\vec{q}'} = \frac{(2\mu/\hbar)^{3/2}}{4\pi\omega_i\omega_s\omega_B} \langle v | \vec{\epsilon} \cdot \vec{p} | c \rangle D_{jj} \langle c | \vec{\epsilon}' \cdot \vec{p} | v \rangle \times \{ [(\omega_g - \omega_s)^{1/2} - (\omega_g - \omega_i)^{1/2}] + [(\omega_g + \omega_i)^{1/2} - (\omega_g + \omega_s)^{1/2}] \}, \quad (3.18)$$

where $\omega_g = E_g/\hbar$ and $\mu^{-1} = m_e^{-1} + m_h^{-1}$.

From Eqs. (3.16) and (3.17) we get for the ratio of the intensity of light scattered by bound and continuum phonons

$$I_B/I_C = \sum_j Z_{jj} / \sum_j \int \rho_{2,jj}^{(c)}(\omega) d\omega. \quad (3.19)$$

In obtaining Eq. (3.19) we have taken the factor $(n_{\omega_j} + 1)^2/\omega_j^2$ outside the integral in Eq. (3.17). It follows from the definition of N_s that

$$\sum_j \int \rho_{2,jj}^{(0)}(\omega) d\omega = 3N_s. \quad (3.20)$$

Substituting Eqs. (2.14) and (3.20) into Eq. (3.19), we obtain the theoretical estimate

$$\frac{I_B}{I_C} \approx \frac{Z_{\text{total}}}{3N_s - Z_{\text{total}}} = 0.087. \quad (3.21)$$

This estimate should be compared with the experimental data of Solin and Ramdas,³ which give

$$I_B/I_C \approx 0.05 \quad (3.22)$$

obtained by taking the integrated intensities of the Raman spectrum. The good agreement between these values of I_B/I_C indicates that the anomalous peak at 2666.9 cm⁻¹ of diamond is adequately explained by the two-phonon bound-state model as proposed by Cohen and Ruvalds.¹ Both the size of the splitting from the top of the continuum and the Raman scattering intensity of the bound state are in quantitative agreement with experiment.

IV. CONCLUSION

The present results provide further support for the theoretical suggestion^{1,4} which attributes the sharp peak in the Raman spectrum observed in diamond to the formation of two-phonon bound states. Furthermore, our results take into account explicitly the relative contributions of LO and TO phonons to the bound-state strength and indicate that they are comparable in magnitude, even though TO phonons are more dispersive.

⁷Research supported in part by the National Science Foundation Grant No. NSF-GH-32747.

¹M. H. Cohen and J. Ruvalds, Phys. Rev. Lett. **23**, 1378 (1969).

²R. S. Krishnan, Proc. Indian Acad. Sci. **24**, 25 (1946).

³S. Solin and A. K. Ramdas, Phys. Rev. B **1**, 1687 (1970).

⁴J. Ruvalds and A. Zawadowski, Phys. Rev. B **2**, 1172

(1970).

⁵K. L. Ngai and E. J. Johnson, Phys. Rev. Lett. **29**, 1607 (1972).

⁶B. A. Weinstein and M. Cardona, Phys. Rev. B **8**, 2795 (1973).

⁷A. K. Ganguly and K. L. Ngai, Phys. Stat. Solidi (to be published).

⁸J. L. Warren, J. L. Yarnell, G. Dolling, and R. A.

- Cowley, Phys. Rev. 158, 805 (1966).
- ⁹J. F. Scott, Phys. Rev. Lett. 21, 907 (1968), and references cited therein.
- ¹⁰G. Leibfried and W. Ludwig, Solid State Phys. 12, 276 (1961).
- ¹¹R. Loudon, Proc. R. Soc. A 275, 218 (1963).
- ¹²K. L. Ngai, Phys. Rev. Lett. 32, 215 (1974).
- ¹³A. Messiah, *Quantum Mechanics* (Wiley, New York, 1965), Vol. II, p. 807.
- ¹⁴A. K. Ganguly and J. L. Birman, Phys. Rev. 162, 806 (1967); D. L. Mills and E. Burstein, Phys. Rev. 188, 1465 (1969).
- ¹⁵A. A. Abrikosov, L. P. Gorkov, and I. E. Dzyaloshinsky, *Methods of Quantum Field Theory in Statistical Physics* (Prentice-Hall, Englewood Cliffs, N.J., 1964), p. 151.